Correspondence

Improvement of the Wall-Current Detector

Since the publication by de Ronde,[1] the construction of the wall-current detector has been modified, resulting in the following improvements:

1) The frequency characteristic has become flatter, within 1.5 db instead of 3 db.
2) The identity of the frequency characteristic for two detectors has become better, within 0.1 db instead of 0.2 db.
3) The sensitivity has become higher, a minimum sensitivity of 10 mv/mw for 1N26 for a detector load of 1 MΩ at a level not exceeding 10 mw.

Due to the modification, the reflection coefficient has become twice as large—$|R| \leq 0.01$ instead of ≤ 0.005—which is still rather low.

The new construction can be seen in Fig. 1. Only the modifications are indicated. Fig. 2 shows the frequency characteristic obtained by the old and new construction, both used with the same sweep oscillator and diode.

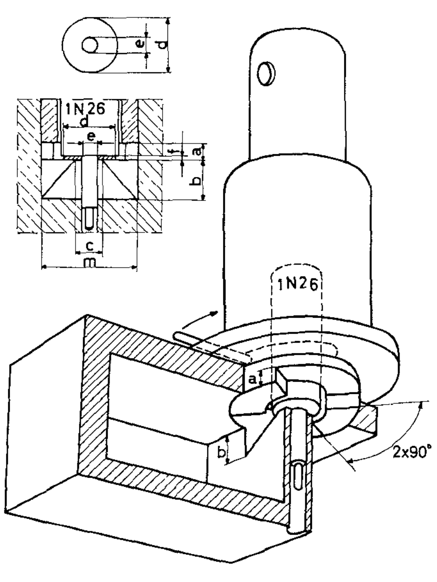

Fig. 1—Internal construction of the improved wall-current detector. $a=2.0$. $b=4.0$ $c=\phi 3.0$. dimensions of mica disk. $d=\phi 5.5$. $e=\phi 1.6$. $f=0.1$. All dimensions in mm.

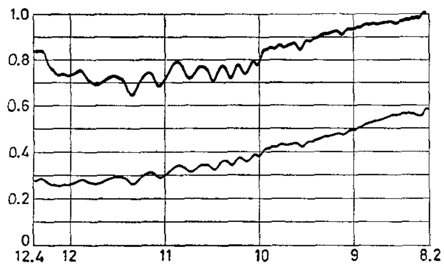

Fig. 2—Frequency characteristic of first and improved wall-current detector for the 8.2–12.4 Gc band. 1.0 corresponds to 100 mv dc voltage of the 1N26 diode over a 1 MΩ load. Lower curve: first wall-current detector. Upper curve: improved wall-current detector.

Influences on the Frequency Characteristic

With the old construction, the sensitivity diminished at higher frequencies. It is reasonable that this will be improved with the *new construction*, especially the dimensions b, c and m. The sensitivity will become higher when b and m are larger. If they are too large, resonance starts at the highest microwave frequency. This can be damped more or less by increasing the losses in the LC circuit, formed by the opening in the wall and the condenser C of the 1N26 diode. The simplest way proved to be to increase the losses of C, which could be done artificially by inserting a small disk of mica—coated with a resistive layer—in front of this condenser. 500 Ω per square proved to be the best value for this layer. It improved the identity slightly and enlarged the sensitivity around the center of the X band. With a lower value a flatter frequency characteristic is obtained, but it has so much influence that the identity is easily spoiled. It will be evident that maximum identity between two detectors is obtained when close tolerances for the dimensions of the LCR circuit are maintained. The inner conductor of the diode is in spring contact with the wall, which for this purpose is split. With the rotary part of the compensation circuit,[1] the slope of the frequency characteristic can be varied about 10 per cent.

If the same absorbing disk had also been used in the old construction, the same flatness, however, but about half the sensitivity of the improved wall-current detector, could have been achieved. As the influence of the resistivity on the frequency characteristic is much greater, this solution is not preferable if maximum identity is wanted.

Concluding, we may say there is no point in trying to get an absolutely flat frequency characteristic as any sweep oscillator has a different response. Influences *from outside* the wall-current detector on the frequency characteristic are the load and the energy level. Both vary the impedance Z_D of the diode and in this way influence the characteristic. A load not smaller than about 50 kΩ, and a level not exceeding 10 mw, are necessary to obtain the above mentioned results of flatness, identity and sensitivity. Higher precision has therefore been achieved by automatic measurement, of which a publication will follow.[2] If one wall-current detector has been used as a leveler, the output of a H/P 686 C sweep oscillator, measured with another detector, could be flat within ±0.1 db.

A Total Reflection Wall-Current Detector

Besides a wall-current detector with hardly any reflection, one with total reflection has been made. By placing a wall-current detector in the middle of the end wall of a quarter wavelength-short, and with $b=0.5$ mm, about the same frequency characteristic has been obtained. In addition, the sensitivity has become about four times as high, which corresponds to the double current for square-law detection. Such a detector might be very useful to investigate the transmission properties of n-ports which may be very important for automatic measurements.

F. C. de Ronde
Philips Research Labs.
N. V. Philips Gloeilampenfabrieken
Eindhoven, The Netherlands

Manuscript received June 26, 1964.

[1] F. C. de Ronde, "A universal wall-current detector," IEEE Trans. on Microwave Theory and Techniques, vol. MTT-12, pp. 112–117; January, 1964.

[2] F. C. de Ronde, "A precision X-band reflectoscope. Automatic full-band display of reflection coefficient," to be submitted for publication in IEEE Trans. on Microwave Theory and Techniques.

Multiband Cavity for High Temperature Plasma Measurements

The design of microwave cavities for investigating high temperature arc plasmas must provide for adequate cooling, vacuum sealing, high Q, minimum disturbance to gas flow and general versatility. In a typical plasma experiment[1,2] (shown in Fig. 1) ionized argon gas flows through a one centimeter circular pipe formed by a stack of insulated water cooled copper disks. Ionization is maintained thermally by an electric arc burning along the pipe axis. The heat transferred to the walls may be 100 w/cm^2 and central temperatures exceed 8000°K at currents in the neighborhood of 100 a. The cavity is located in the stack so that the gas flow is along its axis.

Manuscript received July 6, 1964. The work presented in this paper was sponsored by the National Science Foundation.

[1] H. W. Emmons, "Recent developments in plasma heat transfer," in "Modern Developments in Heat Transfer," Academic Press, Inc., New York, N. Y.; 1963.

[2] H. W. Emmons and R. I. Land, "Poiseuille plasma experiment," *Phys. Fluids*, vol. 5, pp. 1489–1500; December, 1962.

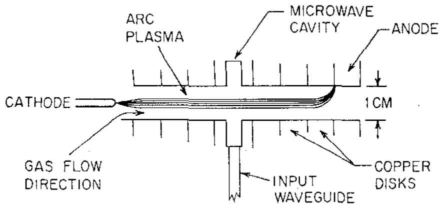

Fig. 1—Section of the plasma apparatus showing the microwave cavity.

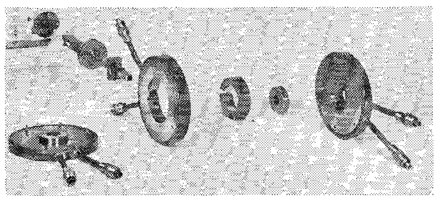

Fig. 2—Exploded view of the microwave cavity.

The mechanical complexity introduced by the requirements of water cooling and vacuability make the construction of separate cavities for each frequency undesirable. A single circular cylindrical cavity shell is described below which can by means of insert rings and plugs operate over a frequency range greater than 2 to 1 (36 to 88 Gc). The assembly has considerable mechanical strength. The cavity is short enough to avoid serious fluid flow problems but long enough to achieve a reasonable Q. Both the iris size and position can be changed to allow a variety of modes to be excited.

The cavity assembly is shown partially dismantled in Fig. 2. The cavity shell consists of three parts: a body 3 inches in diameter and 0.438 inch thick and two end plates each 3 inches in diameter and $\frac{1}{16}$ inch thick. All are copper with 0.5 per cent tellurium added for ease of machining. Copper provides both the high thermal conductivity and when polished the high surface electrical conductivity desired. Water channels milled in each part are connected via $\frac{3}{16}$ inch copper tubing to $\frac{1}{4}$ inch polyflow fittings. Each end plate is secured to the body by six screws which clamp a Parker 2-38 O-ring-vacuum seal. The actual microwave working surfaces are formed by an insert ring which reduces the diameter from 1.5 inches to that desired and two insert plugs which attach with screws to the end plates and fit inside the insert rings to reduce the length.

In the foreground of Fig. 2 one sees from right to left an end plate, insert plug, insert ring, cavity body, and the other end plate with insert plug attached. Behind is shown the waveguide which is built up to fit the rectangular hole in the body. The coupling iris is drilled in a 0.010 inch brass plate which is soldered directly onto the end of the input waveguide. This waveguide is inserted through the hole in the body, past the slotted ring until it seats against the plugs. A sliding flange shown mounted on the waveguide is then tightened down against a small O-ring (stretched over the waveguide). This arrangement affords a vacuum seal to the waveguide and also holds it in place. For nonsymmetrical excitation the waveguide is located as far off the cavity midplane as possible and the iris is moved off the guide center if necessary to obtain the appropriate coupling. While this scheme is not perfect it works well enough to allow excitation of TE_{nm2} modes with adequate coupling.

The theoretical Q_0 for the TE_{011} mode at 38 Gc (neglecting end plate holes) is about 7000. The experimental Q_0 is found to be greater than 2000. At some frequencies this exceeds the wavemeter Q used in spite of the cavity's large end plate holes and pancake shape. In the smallest cavity employed, the plasma need leap across a gap of only just over $\frac{1}{16}$ inch.

Data reproducibility is excellent. In actual use measurements were taken with the cavity. It was then dismantled and assembled with a different set of inserts. When it was reassembled in its original form, the original data were reproduced exactly (within experimental error).

William T. Maloney
Div. of Engrg. and Appl. Phys.
Harvard University
Cambridge, Mass.

Radiation Characteristics for a Magnetic Line Source in Homogeneous Electron Plasmas

The radiation characteristic of a magnetic line source in an anisotropic compressible electron plasma was discussed in a recent paper by Seshadri.[1] In Seshadri's paper an excessive amount of effort is devoted to evaluating certain integrals occurring in the Fourier transform solutions of the single-fluid magnetohydrodynamic equations. The following discussion presents a greatly simplified method of evaluating the appropriate integrals describing the "optical" and "plasma" modes of radiation.

The time harmonic ($\exp -i\omega t$) equations for the single-fluid compressible system may be formulated as

$$\nabla \times E - i\omega\mu_0 H = -J_m \tag{1}$$

$$\nabla \times H + i\omega\epsilon_0 E = NeV \tag{2}$$

$$-i\omega m N_0 V = Ne(E + V \times B_0) - \nabla P \tag{3}$$

$$a^2 m N_0 \nabla \cdot V = i\omega P. \tag{4}$$

The notation utilized in (1)–(4) is that which Seshadri chose in his formulation. Furthermore, we now restrict our attention to a magnetic line source parallel to the y-axis of a right handed system (x, y, z). Imposing this constraint to (1)–(4) and applying Fourier transform theory, we obtain the integral equations for H_y and P (see Seshadri[2]).

$$H_y(x, z) = \frac{i\omega\epsilon_0\epsilon J_0}{4\pi^2\epsilon_1}\int_{-\infty}^{\infty}\int_{-\infty}^{\infty} \cdot \frac{(\eta^2 + \zeta^2 - k_a^2)e^{i(\zeta x+\eta z)}}{\Delta}\, d\eta d\zeta \tag{5}$$

$$P(x, z) = \frac{i\omega X B_0\epsilon_0\epsilon}{4\pi^2(1 - X)\epsilon_1}\int_{-\infty}^{\infty}\int_{-\infty}^{\infty} \cdot \frac{(\eta^2 + \zeta^2)e^{i(\zeta x+\eta z)}}{\Delta}\, d\eta d\zeta \tag{6}$$

where

$$X = \frac{\omega_p^2}{\omega^2}, \quad Y = \frac{\omega_g}{\omega}, \quad \epsilon = \epsilon_1^2 + \epsilon_2^2$$

$$\epsilon_1 = \frac{1 - X - Y^2}{1 - Y^2}, \quad \epsilon_2 = \frac{XY}{1 - Y^2},$$

$$\Delta = (\eta^2 + \zeta^2 - k_{mp}^2)(\eta^2 + \zeta^2 - k_{m0}^2) \cdot \left[\frac{(1 - X + Y)(1 - X - Y)}{(1 - X)(1 - X - Y^2)}\right],$$

k_{m0}^2 and k_{mp}^2 are roots of $P(\lambda) = 0$, where

$$P(\lambda) = \lambda^4 - (\omega^2/c^2 + \omega^2/a^2)(1 - X - Y^2) + (\omega^2/a^2)(\omega^2/c^2)[(1 - X)^2 - Y^2],$$

$$k_a^2 = \frac{\omega^2}{a^2}\left[\frac{(1 - X)^2 - Y^2}{1 - X}\right],$$

$$k_e^2 = \omega^2/c^2\left[\frac{(1 - X)^2 - Y^2}{1 - X - Y^2}\right].$$

Unfortunately, Seshadri chose to evaluate the integrals in (5) and (6) in rectangular coordinate systems as given. In so doing, he encountered multivalued integrands which complicated the evaluation of the magnetic field and hydrostatic pressure in the plasma. The following evaluation of the integrals provides a rather simple method for the description of the radiation characteristic of the line source.

The integrals are defined as

$$I_1 = \int_{-\infty}^{\infty}\int_{-\infty}^{\infty} \frac{(\eta^2 + \zeta^2 - k_a^2)e^{i(\zeta x+\eta z)}}{\Delta}\, d\eta d\zeta, \tag{7}$$

$$I_2 = \int_{-\infty}^{\infty}\int_{-\infty}^{\infty} \frac{(\eta^2 + \zeta^2)e^{i(\zeta x+\eta z)}}{\Delta}\, d\eta d\zeta. \tag{8}$$

Transforming both real-space and transform-space variables to polar coordinates, we recognize the integration with respect to the angular variable as an identity for the Bessel functions and obtain[3]

$$I_1(\rho) = 2\pi\int_0^{\infty} \frac{(\lambda^2 - k_a^2)\lambda J_0(\lambda\rho)d\lambda}{\Delta(\lambda)} \tag{9}$$

$$I_2(\rho) = 2\pi\int_0^{\infty} \frac{\lambda^3 J_0(\lambda\rho)d\lambda}{\Delta(\lambda)}. \tag{10}$$

We now make use of complex function theory, substitute Hankel functions for the

Manuscript received May 21, 1964; revised July 27, 1964.

[1] S. R. Seshadri, "Excitation of Plasma Waves in an Unbounded Homogeneous Plasma by a Line Source," IEEE Transactions on Microwave Theory and Techniques, vol. MTT-11, pp. 39–49; January, 1963.

[2] *Ibid.*, see (35) and (36) on p. 43.

[3] E. Jahnke and F. Emde, "Tables of Functions," Dover Publications, New York, N. Y.; 1945.